Amelioration of progressive renal injury by genetic manipulation of *Klotho* gene

Yoshisuke Haruna*, Naoki Kashihara*†, Minoru Satoh*, Naruya Tomita*, Tamehachi Namikoshi*, Tamaki Sasaki*, Toshihiko Fujimori‡, Ping Xie§, and Yashpal S. Kanwar§

*Division of Nephrology, Department of Internal Medicine, Kawasaki Medical School, Kurashiki, Okayama 701-0192, Japan; ‡Department of Pathology and Tumor Biology, Kyoto University Graduate School of Medicine, Kyoto 606-8501, Japan; and §Department of Pathology, Northwestern University Medical School, Chicago, IL 60611

Klotho, an antiaging gene with restricted organ distribution, is mainly expressed in the kidney tubules; the mutant mice have shortened life span, arteriosclerosis, anemia, and osteoporosis, features common to patients with chronic renal failure. Conceivably, the reduction of the *Klotho* gene expression may contribute to the development of kidney failure; alternatively, its overexpression may lead to the amelioration of renal injury in an ICR-derived glomerulonephritis (ICGN) mouse model with subtle immune complex-mediated disease. To address this issue, four different strains of mice were generated by cross-breeding: ICGN mice without the *Klotho* transgene (ICGN), ICGN mice with the *Klotho* transgene (ICGN/klTG), wild-type mice with the *Klotho* transgene (klTG), and wild-type mice without the *Klotho* transgene (control). At 40 weeks old, the survival rate was ≈30% in ICGN mice, and ≈70% in the ICGN/klTG group. This improvement was associated with dramatic improvement in renal functions, morphological lesions, and cytochrome *c* oxidase activity but a reduction in β-galactosidase activity (a senescence-associated protein), mitochondrial DNA fragmentation, superoxide anion generation, lipid peroxidation, and Bax protein expression and apoptosis. Interestingly, improvement was seen in both the tubular and glomerular compartments of the kidney, although *Klotho* is exclusively confined to the tubules, suggesting that its gene product has a remarkable renoprotective effect by potentially serving as a circulating hormone while mitigating the mitochondrial oxidative stress.

aging | glomerulonephritis | oxidative stress | tubular interstitial disease

Fig. 1. Kaplan–Meier curves reflecting survival for different strains of mice. In the ICGN group, the survival rate was ≈30% at 40 weeks of age, whereas it was restored to ≈70% in the ICGN/klTG group with the overexpression of the *Klotho* gene. In the control and klTG groups, the survival rate was >90%. *, *P* < 0.01 compared with the ICGN group (*n* = 20).

The *Klotho* gene was originally identified by insertional mutagenesis, and it encodes a 130-kDa transmembrane protein that shares sequence homology with β-glucosidase (1). The gene is predominantly expressed in the kidney and, to a lesser extent, in the brain and reproductive and endocrine organs. Its deletion in mice ($Kl^{-/-}$) results in the development of a syndrome resembling human aging, including shortened life span, growth retardation, infertility, arteriosclerosis, skin and muscle atrophy, osteoporosis, and pulmonary emphysema (1). Conversely, overexpression of the *Klotho* gene extends the life span in mice (2). Although $kl^{-/-}$ mice do not show any overt renal abnormalities, the *Klotho* mRNA expression in the kidneys has been shown to be greatly reduced in patients with chronic renal failure (3). Notably, most of the features of *Klotho* gene-deleted mice are similar to those of the patients with chronic renal failure. In addition, *Klotho* gene expression has been found to be reduced in acute renal failure in ischemia-reperfusion injury murine models (4). These findings would imply that the reduction of Klotho protein may be relevant to the pathophysiology of renal failure. However, little is known concerning whether Klotho protein itself could exert an ameliorative effect on a diseased kidney to preserve its renal functions and thus could serve as a therapeutic target in various renal diseases.

To address this issue, the *Klotho* gene was introduced into a mouse model of glomerulonephritis carrying a mutation in the *Tensin2* gene (5)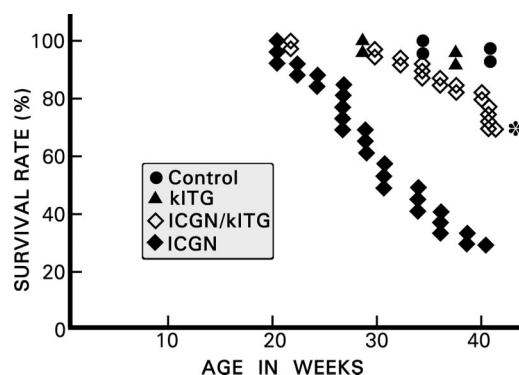. This mutant strain of mice is derived from outbred ICR mice that spontaneously develop nephrotic syndrome and progressive renal injury leading to chronic kidney failure (6). The strain is described as ICR-derived glomerulonephritis (ICGN), and the tubulointerstitial compartment of these mice is also adversely affected besides having a proliferative form of mild glomerulonephritis.

Results

Amelioration of Renal Injury and Extended Life Span by *Klotho* Gene Overexpression in ICGN Mice. Increased urinary albumin excretion was observed as early as 1 week of age in ICGN mice. At 5 weeks, the urinary albumin excretion was significantly increased in ICGN mice compared with controls (3.0 ± 0.03 vs. 22.3 ± 2.18 mg/day), and it more than doubled by 40 weeks (from 22.3 ± 2.18 to 52.6 ± 5.39 mg/day). Some of the ICGN mice developed generalized edema and ascites. Along with the development of proteinuria, renal functions also deteriorated in ICGN mice, as indicated by increased blood urea nitrogen levels (25.3 ± 2.6 vs. 63.4 ± 10.2 mg/dl). *Klotho* gene overexpression significantly reduced proteinuria in ICGN mice with the *Klotho* transgene (ICGN/klTG; from 52.6 ± 5.39 to 22.5 ± 2.19 mg/day) and improved blood urea nitrogen levels at 40 weeks of age (from 63.4 ± 10.2 to 34.3 ± 3.6 mg/dl). Similar corrections were seen in serum creatinine values in
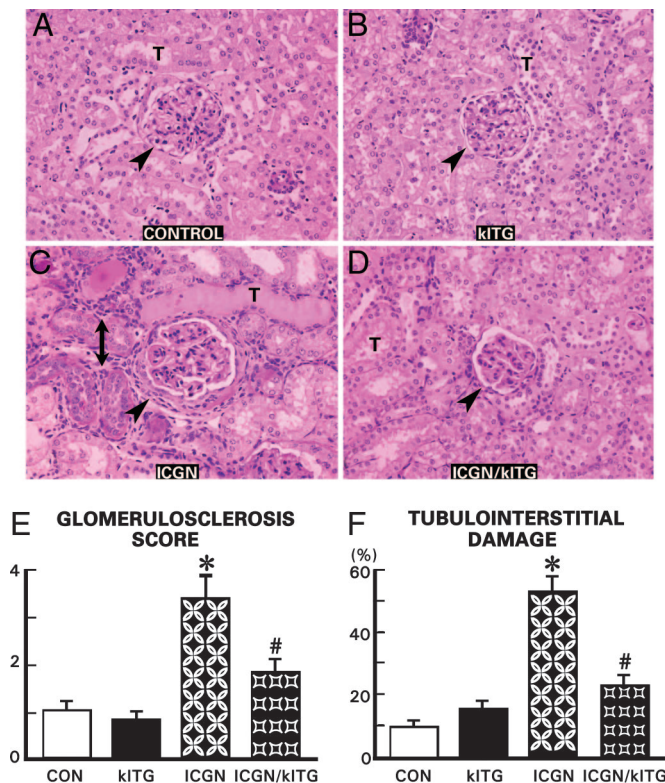
MEDICAL SCIENCES

Fig. 2. Representative kidney sections stained with periodic acid-Schiff from various strains of mice (*A–D*), reflecting glomerulosclerosis score (*E*) and the percentage of tubulointerstitial damage (*F*). In the ICGN group, the glomeruli were relatively large and hypercellular and had thickened loops (*C*, arrowhead) compared with the control and klTG groups (*A* and *B*). Also, tubular atrophy, thickening of the basement membranes, and influx of mononuclear cells was seen (*C*, double-headed arrow). (*D*) The glomerular hypercellularity and tubulointerstitial cellular infiltrates were notably lessened in the ICGN/klTG group with the overexpression of the *Klotho* gene. (*E* and *F*) A remarkable degree of glomerulosclerosis and tubulointerstitial damage was seen in the ICGN group, which was partially reversed in the ICGN/klTG group. (*E*) Results are given as the mean ± SEM. *, $P < 0.05$ compared with the control group; #, $P < 0.05$ compared with the ICGN group ($n = 8$). T, tubule.
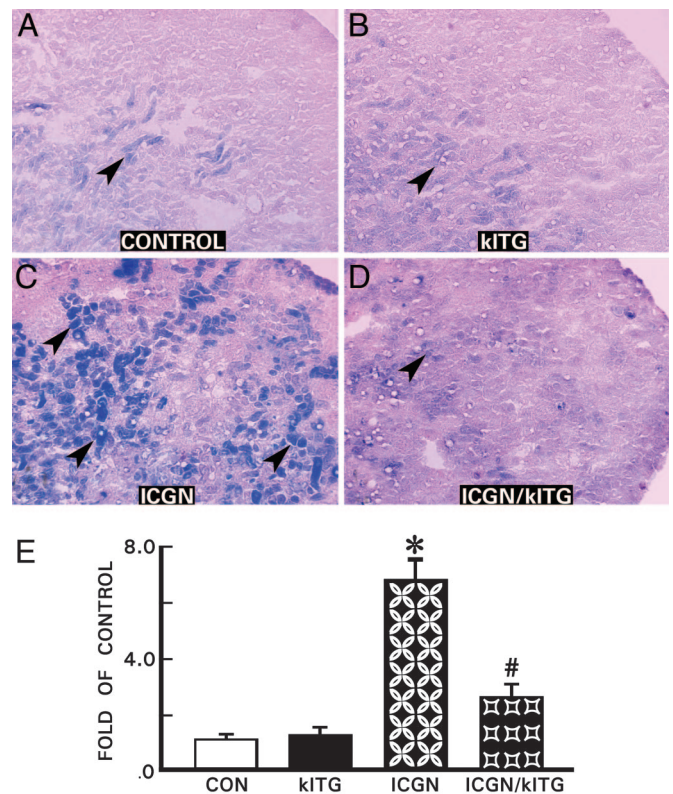

Fig. 3. Representative kidney sections exhibiting cellular senescence associated β-galactosidase activity in various strains of mice. An intense activity (blue staining) was observed in the kidney tubules of the ICGN group (*C*, arrowheads), which was notably reduced with the overexpression of the *Klotho* gene (*D*). A mild basal β-galactosidase activity was seen in the control and klTG groups (*A* and *B*). (*E*) Percentages of in β-galactosidase-positive areas were measured, and the results are presented as the mean ± SEM. *, $P < 0.05$ compared with the control group; #, $P < 0.05$ compared with the ICGN group ($n = 8$).

ICGN vs. ICGN/klTG mice (from 0.26 ± 0.05 to 0.18 ± 0.01 mg/dl). By 40 weeks of age, 16 of 28 mice died in the ICGN group, whereas only 8 mice died in the ICGN/klTG group (Fig. 1). Overall, the survival rate was ≈30% in the ICGN group, and it improved significantly (≈70%, $P < 0.05$) for the ICGN/klTG group.

Both control and klTG groups showed no abnormalities in the glomerulus and tubulointerstitium at 40 weeks of age (Fig. 2 *A* and *B*). In the ICGN group, the glomeruli were hypercellular, had thickened capillary loops, and expanded mesangial regions (Fig. 2*C*, arrowhead). Varying degrees of sclerosis were found in some of the glomeruli of ICGN mice, which was ≈2-fold higher compared with the ICGN/klTG group (Fig. 2*E*). Tubulointerstitial changes in ICGN mice included tubular atrophy, mononuclear cell infiltration, fibrosis, and thickened basement membranes (Fig. 2*C*, double-headed arrow). Foci of tubular dilatation were also observed. Overexpression of the *Klotho* gene reduced the development of the glomerular and tubulointerstitial changes in ICGN/klTG mice, although residual mild glomerular proliferation and thickening of the capillary loops persisted (Fig. 2*D*, arrowhead). No major foci of tubular atrophy or interstitial cellular infiltrates were seen. Overall, the tubulointerstitial damage was reduced by ≈50% in the ICGN/klTG group (Fig. 2*F*).

Accelerated Cellular Senescence in Diseased Kidneys. β-Galactosidase activity, a marker of cellular senescence, was evaluated in renal

tissues (7). Strong and widespread β-galactosidase activity (blue) was observed in the renal cortex and medulla in the ICGN group of mice (Fig. 3*C*, arrowheads). Blue staining was localized mainly in the cytoplasm of the tubular epithelial cells. Weak staining was also seen in the glomerular cells. Overexpression of the *Klotho* gene suppressed the β-galactosidase activity by ≈70% in renal tissues of ICGN/klTG mice (Fig. 3 *D* and *E*). A mild background activity was also observed in the renal tissues of control and klTG mice; however, the intensity of staining was relatively weak, and the positive areas were restricted to renal medulla (Fig. 3 *A* and *B*, arrowheads). These findings imply that cellular senescence was accelerated in the ICGN mice and that overexpression of the *Klotho* gene could suppress manifestation of senescence-associated phenotype in the diseased kidney.

Partial Restoration of Mitochondrial Functions by *Klotho* Gene Overexpression. By electron microscopy, the mitochondria were relatively small in the ICGN group compared with the ICGN/klTG group of mice, in which they were large and had an oblong shape (Fig. 4 *A* vs. *B*). However, overt ultrastructural abnormalities were not observed in the mitochondrial cristae (arrows). Nevertheless, there were significant differences in the cytochrome *c* oxidase activity among various strains of mice. Cytochrome *c* oxidase is a large transmembrane protein that acts as a terminal acceptor in the electron transport chain. It is one of the key enzymes modulating mitochondrial functions, and its activity was assessed by enzyme histochemical method (8). Strong cytochrome *c* oxidase activity
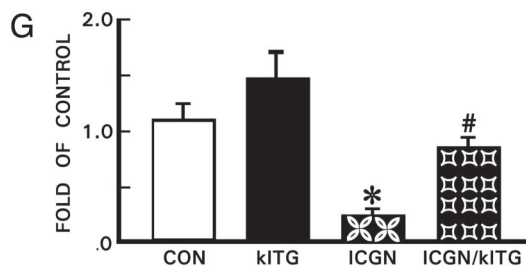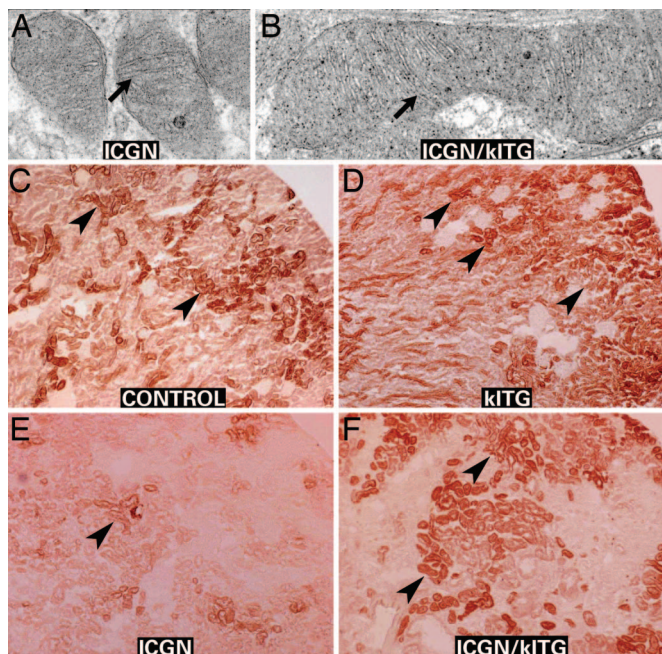
Fig. 4. Representative kidney sections depicting mitochondrial changes (*A* and *B*) and cytochrome *c* oxidase activity (brown reaction product) (*C–F*) in various strains of mice. Mitochondria were smaller in the ICGN group compared with those of ICGN/klTG mice; however, the cristae were normal (arrows). An intense cytochrome *c* oxidase activity was present in the control and klTG groups (arrowheads). Activity was markedly reduced in the ICGN group, and it was largely restored in the ICGN/klTG group. The percentages of positive areas were measured, and the results are presented as the mean ± SEM (*G*). *, $P < 0.05$ compared with the control group; #, $P < 0.05$ compared with the ICGN group ($n = 8$).

(brown) was observed to be widely expressed in the renal cortex, mainly in the tubular epithelium, in control group of mice (Fig. 4*C*, arrowhead). The cortical activity of enzyme in ICGN mice was significantly suppressed compared with age-matched control or klTG mice (Fig. 4 *E* vs. *C* and *D*). Overexpression of the *Klotho* gene normalized the enzyme activity to a large extent (Fig. 4 *F* and *G*), indicating that mitochondrial electron chain transport system was restored, at least partially, by Klotho protein.

Reduction of Mitochondrial DNA Damage by Klotho Protein. Fragmentation of mtDNA in renal tissues, possibly related to oxidative stress, was evaluated by PCR (9). Random DNA lesions are more likely to hamper the progression of the polymerase and decrease PCR amplification for long DNA fragments than short fragments. The 8636-bp amplification product of mtDNA was decreased in the ICGN group, whereas amplification of the 316-bp fragment was largely unaffected in the ICGN and other strains of mice (Fig. 5*A*). As a result, the ratio of 8636/316-bp product intensity was decreased by ≈80% in the renal tissue of the ICGN group compared with the control or klTG groups. The mtDNA damage revealed by this method was remarkably reduced in ICGN/klTG mice (Fig. 5*B*),
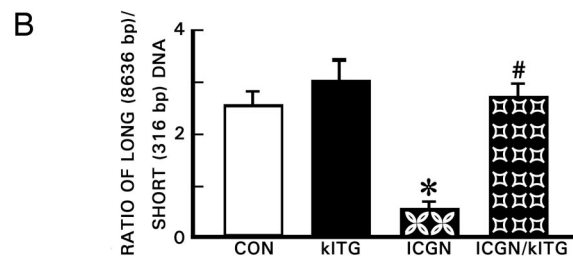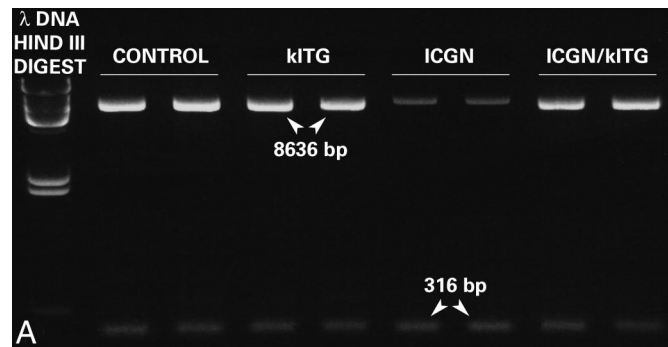

Fig. 5. Electrophoretogram of mtDNA isolated from renal tissues of various strains of mice. The mtDNA damage was evaluated by the long PCR technique. (*A*) In the ICGN mice, intensity of 8636-bp product was reduced compared with the 316-bp PCR product, suggesting damage to higher molecular DNA. The damage was restored in the ICGN/klTG strain of mice, indicating the *Klotho* gene being protective of mtDNA. (*B*) Densitometer readings of the ratio of 8636/316-bp band intensity are given as the mean ± SEM. *, $P < 0.05$ compared with the control group; #, $P < 0.05$ compared with the ICGN group ($n = 8$).

suggesting that the Klotho protein exerts a protective effect on the renal injury associated with mtDNA damage.

Reduction of Oxidative Stress Was Decreased by Klotho Protein. Superoxide anion production in renal tissue was evaluated by dihidroethidium conversion to ethidium and imaged by confocal laser-scanning microscopy (10). A strong dihidroethidium fluorescence was seen in the ICGN group (Fig. 6*A*), indicating superoxide anion production. The dihidroethidium fluorescence was suppressed in ICGN/klTG mice almost to control levels (Fig. 6*B*). Immunostaining was used to evaluate 4-hydroxy-2-nonenal-modified protein expression in renal tissue. The 4-hydroxy-2-nonenal-positive cells, a marker of lipid peroxidation, were detected in glomeruli and tubular epithelia in ICGN mice (Fig. 6*C*, arrowheads), and such immunoreactivity was not observed in the control and klTG mice. The immunoreactivity was remarkably inhibited in the renal tissues of ICGN/klTG mice (Fig. 6*D*). Average urinary excretion of 8-hydroxydeoxyguanosine, a marker of oxidative DNA damage, was significantly increased in the ICGN group but was notably suppressed in the ICGN/klTG group (Fig. 6*E*), indicating that *Klotho* gene overexpression globally reduced the oxidative damage.

Assessment of Apoptosis and Apoptosis-Related Proteins' Expression. Renal tissues from 40-week-old mice were harvested and subjected to TUNEL assay for *in situ* detection of apoptotic cells (11). A drastic increase in the number of apoptotic nuclei was observed in the ICGN group (Fig. 7*F*). Apoptosis was reduced to basal levels with the overexpression of the *Klotho* gene in ICGN/klTG mice, similar to that in the control and klTG groups. Expression of antiapoptotic Bcl-2 protein was notably down-regulated, whereas that of apoptotic Bax protein was increased in the kidneys of ICGN group mice (Figs. 7 *A* and *B*). Overexpression of the *Klotho* gene partially corrected the altered expression of Bcl-2 and Bax (Figs. 7

MEDICAL SCIENCES

Fig. 6. Representative kidney sections from various strains of mice depicting superoxide anion production (*A* and *B*) and lipid peroxidation (*C* and *D*), and urinary excretion of 8-hydroxy-deoxyguanosine (*E*). An intense UV fluorescence in samples of ICGN mice (*A*) was detected, indicating generation of superoxide anion by conversion of dihidroethidium to ethidium, which was drastically reduced in the ICGN/klTG group (*B*). Lipid peroxidation in glomerular and tubular cells of the ICGN mice was detected by employing anti-4-hydroxy-2-nonenal polyclonal antibody (*C*, arrowheads), but it was undetectable in the ICGN/klTG group (*D*). (*E*) The oxidative modification of nucleic acid was assessed by urinary excretion of 8-hydroxy-deoxy-guanosine (8OH-dG). The relatively high excretion was observed in the ICGN group, and it was reduced by 5- to 6-fold in the control, klTG, and ICGN/klTG groups. (*E*) Results are given as the mean $\pm$ SEM. $*$, $P < 0.05$ compared with the control group; #, $P < 0.05$ compared with the ICGN group ($n = 8$).

D and *E*). The α-tubulin expression was similar in different strains of mice (Figs. 7*C*).

Discussion

Aging, a normal physiological process, is associated with phenotypic changes in mammals, which at times lead to functional deterioration in various organ systems (12). It seems that the changes occur simultaneously in various organ systems, including the kidney, that are characterized by diminution of renal mass and functions. During this so-called "renal senescence," other comorbid conditions, such as arteriosclerosis, diabetes mellitus, hypertension, etc., also contribute to progressive chronic renal failure with down-regulation of *Klotho* mRNA (13). Conceivably, amelioration of comorbid conditions would be expected to lengthen the life span. This contention is supported by the present investigation in which an increased survival rate was observed in ICGN mice with the overexpression of the *Klotho* gene (Fig. 1). Alternatively, one may suggest that it is the overexpression of the *Klotho* gene that led to the improvement in renal functions and correction of phenotypic alterations in the glomerular and tubulointerstitial compartments (Fig. 2). Certainly, the finding that there was a decrease in senescence-associated β-galactosidase activity in ICGN/klTG mice (Fig. 3) would be in

Fig. 7. Immunoblot analyses of Bcl-2, Bax, α-tubulin (*A–E*) and extent of apoptosis (*F*) in renal tissues of various strains of mice. A decreased expression of Bcl-2, an antiapoptotic protein, and increased expression of Bax, a proapoptotic protein, was observed in ICGN mice; the expression was partially reversed by overexpression of the *Klotho* gene in the ICGN/klTG group (*A*, *B*, *D*, and *E*). The α-tubulin expression was similar in all of the strains (*C*). By TUNEL assay, a marked apoptosis was observed in the ICGN group, and it was suppressed by overexpression of the *Klotho* gene in the ICGN/klTG mice (*F*). A minimal degree of apoptosis was observed in the control and klTG groups. The results are given as the mean $\pm$ SEM (*D–F*). $*$, $P < 0.05$ compared with the control group; #, $P < 0.05$ compared with the ICGN group ($n = 8$).

line with the latter notion that the Klotho protein exerted an ameliorative effect in this murine model of subtle immune-complex-mediated injury. The latter injury at times is regarded as also reflective of the senescence process because several systemic autoimmune diseases evolve during the second to fourth decades and progress with age in humans (12).

Although the *Klotho* gene encodes a type I membrane protein, its effects seem to be wide spread and systemic rather than cell-autonomous where it is primarily expressed (14) and thus could act as a circulating factor like another endogenously produced hormone by the kidney, erythropoietin. In this regard, the literature data indicate that the N-terminal extracellular domain of the

Klotho protein is shed and secreted into the blood and potentially functions as a humoral factor that modulates the intracellular insulin/insulin-like growth factor 1-signaling cascade, which partly may contribute to the mechanism of extended life span (2). The *Klotho* gene is only one of several known factors, e.g., NO, oxidative stress related to mitochondrial dysfunction, renin–angiotensin system, and cell-cycle proteins and length of telomeres that are relevant to the blood borne circulatory stress of aging. The NO production may be aberrant in $Kl^{-/-}$ mice because they exhibit impaired vasodilation (15) and angiogenesis (16) with the loss of the protective effect of the Klotho protein on the cardiovascular system (17). Remarkably, *in vivo Klotho* gene delivery increases endothelial-derived NO production and abrogates cardiovascular complications in a rat model with multiple atherogenic risk factors (18). Human studies indicating NO deficiency contributing to cardiorenal vascular complications also emphasize the relevance of Klotho protein as a potential therapeutic agent (19). Besides NO, conceivably other factors including oxidant stress related to mitochondrial dysfunctions, may also be pertinent to the pathobiology of the *Klotho* gene, and these factors were explored in this investigation.

Mitochondria are the main source of cellular ATP and play a critical role in a variety of cellular processes. Of interest here is cytochrome *c* oxidase, an enzyme located in the inner mitochondrial membrane. It catalyses the conversion of molecular oxygen to water and pumps an additional proton across the membrane to establish a chemiosmotic potential that the ATP synthase then uses to synthesize ATP. It is interesting to note that the mitochondria were relatively small in the ICGN group, and cytochrome *c* oxidase activity was markedly diminished (Fig. 4), which points toward mitochondrial dysfunctions in this renal injury model, although their cristae were normal. That these parameters were normalized to a large extent with the overexpression in ICGN/klTG mice suggests that mitochondrial and Klotho functions are interlinked and this reinforces the notion of a relationship of aging with the oxidant stress. The latter is known to induce mtDNA mutations, which are known to accumulate with aging in several tissues of various species (20, 21). In this scenario, the ratio of long- vs. short-bp DNA decreases, which was observed in ICGN mice, and it was reversed by the overexpression of *Klotho* gene (Fig. 5), suggesting that mtDNA fragmentation, possibly induced by oxidant stress, was an integral part, and not an epigenetic event, in the pathogenesiss of renal injury.

Oxidative stress has been implicated in the pathophysiology of a variety of chronic renal diseases (22), including diabetes (23). The nature of reactive oxygen species generated by various mechanisms vary in different forms of renal injury (24, 25). In ICGN mice, the oxidant stress was related to varied mechanisms, including lipid peroxidation and superoxide anion production that, in part, led to the oxidative DNA damage, as reflected by the increased urinary excretion of 8-hydroxydeoxyguanosine (Fig. 6). The oxidant stress, regardless of its origin, was seen remarkably reduced in ICGN/klTG mice, suggesting an antioxidant effect of Klotho protein. The latter has been reported to activate manganese superoxide dismutase via insulin-like growth factor signaling (26). The superoxide dimutase is a mitochondrial enzyme that protects the cells and tissues from oxidative damage (27). In addition, superoxide dimutase mimetic compounds exert similar protective effect in blood vessels during the process of aging (28). The mice deficient in manganese superoxide dismutase exhibit increased reactive oxygen species levels and severe mitochondrial dysfunctions, including mtDNA damage and mutations (29). Conceivably, the accumulation of mtDNA mutations promotes apoptosis (30), and thus, the status of programmed cell death in tissues and its associated proteins (i.e., Bcl-2 and Bax) was investigated. An increased apoptosis with up-regulation of Bax and reduced expression of Bcl-2 was observed in ICGN mice (Fig. 7). The fact that these abnormalities were rectified to a large degree by *Klotho* overexpression suggests that this antiaging factor can reduce oxidant stress, cell death, β-galactosidase activity, and DNA fragmentation; and normalizes cyctochrome *C* oxidase activity suggests that it modulates mitochondrial functions and thus ameliorates renal injury. Note that the improvement in the renal functions in ICGN mice was reflected by the amelioration in the morphology of both the glomerular and tubular compartments, although the *Klotho* gene is mainly expressed in the tubules. Conceivably, correction of tubular pathophysiology may have resulted in the rectification of glomerular lesions, and such an idea had also been proposed by Nath (31) several years ago.

In conclusion, it seems that the antiaging Klotho protein serves as a potential renoprotective humoral factor by reducing mitochondrial oxidative stress and thereby modulating tubulointerstitial and glomerular pathobiology irrespective of the disease process, including the subtle forms of immune-complex-mediated injury.

Materials and Methods

Generation of Animal Models. Transgenic mice that overexpress the *Klotho* gene (*EFmKL46*) were kindly provided by Yo-Ichi Nabeshima (Kyoto University, Japan). These mice express exogenous *Klotho* gene under the control of human elongation factor 1α promoter in addition to its endogenous gene expression; as a result, there is an ≈2-fold higher Klotho protein concentration in the blood (2). By using tail genomic DNA, PCR was performed to confirm exogenous *Klotho* gene. ICGN mice were kindly provided by Junichiro Matsuda (National Institute of Biomedical Innovation, Osaka, Japan). The affected ICGN mice were identified by detection of albuminuria/proteinuria (6). The ICGN mice were crossbred with *Klotho* mice to obtain mice carrying both the *Klotho* transgene and ICGN traits. These mice were cross-bred back with the ICGN mice to obtain four different strains: ICGN/klTG and their littermate controls (ICGN without *Klotho* transgene mice, ICGN; wild-type with *Klotho* transgene mice, klTG; and wild-type without *Klotho* transgene mice, control). Five week-old male klTG, ICGN, ICGN/klTG, and control mice were used with each group consisting of 28 animals. Eight mice in each group were killed with an injection overdose of pentobarbital anesthesia at 40 weeks of age for various studies. The remaining mice were used to measure survival rate by Kaplan–Meier analyses.

Blood and Urinary Measurements. Body weight of mice was measured bimonthly. Urinary protein excretion was measured by using pyrogallol sulfonphthalein method. Blood samples were obtained at the time of death for determination of serum creatinine and blood urea nitrogen by using enzymatic methods. Urinary excretion of 8-hydroxy-deoxy-guanosine was measured by employing competitive ELISA kit (Japan Institute for Control of Aging, Shizuoka, Japan).

Morphometric Evaluation of Renal Tissue. Sections (4 μm thick) were prepared from paraffin embedded tissues and stained with periodic acid-Schiff (PAS) and Masson-trichrome (Sigma-Aldrich, Tokyo, Japan). They were photographed and printed to a final magnification of ×400. The severity of glomerular injury was expressed as a glomerulosclerosis score as follows: 0, no sclerosis; 1, <25% sclerotic changes in glomerulus; 2, 25%–50%; 3, 50%–75%; and 4, >75%. Thirty glomeruli were randomly selected in each tissue section, and an average score was calculated. Severity of tubulointerstitial injury was evaluated by examining 10 fields in randomly selected tissue samples stained with Masson-trichrome. Blue-stained scarred areas were quantified by a color image analyzer (Win ROOF; Mitani, Fukui, Japan). Glomeruli, tubules, and blood vessels of the cortex were excluded. Results were expressed as the percentage of the relative volume of the scanned interstitium. Tissues were also processed for electronmicroscopy to assess the ultrastructural alterations in the mitochondria as described in ref. 11.

Senescence-Associated β-Galactosidase Activity. Senescence-associated β-galactosidase activity was examined as detailed in ref. 7. The percentage of β-galactosidase-positive area was measured by using a color image analyzer. Twenty consecutive fields from each of the mouse kidney were randomly evaluated at a magnification of ×100.

Enzyme Histochemistry of Cytochrome c Oxidase. Histochemical detection of cytochrome c oxidase activity was performed as described in ref. 8. The percentages of positive areas were measured by using a color image analyzer. Twenty consecutive fields of each of the mouse kidney were randomly evaluated at a magnification of ×100.

Immunohistochemistry. Serial sections (4-μm thick) of paraffin-embedded specimens were rehydrated in PBS and subjected to antigen retrieval in a microwave at a setting of 600 W three times, each cycle consisting of 5 min. Mouse anti-4-hydroxy-2-nonenal polyclonal antibody (Alpha Diagnostic, San Antonio, TX) was used as a primary antibody, and detection was carried out by using the DAKO EnVision+ system and diaminobenzidine reagent (Dako Japan, Kyoto, Japan).

Mitochondrial Long PCR Amplification. mtDNA damage was evaluated by PCR. Long-range PCR was used to coamplify long and short mtDNA fragments (9). PCR products were electrophoresed on 1.6% agarose gels and stained with ethidium bromide to visualize the 8636- and 316-bp DNA products. Band intensity was measured with a PhosphorImager (Molecular Dynamics, Sunnyvale, CA) and a ratio between the long and short DNA fragments was calculated.

Extraction of Cytosolic Proteins and Western Blotting. Renal lysates were prepared and proteins extracted (10). Protein samples (100 μg per lane) were subjected to SDSPAGE, followed by immunoblot-ting by using rabbit polyclonal antibodies against Bcl-2, Bax, and α-tubulin (Santa Cruz Biotechnology, Santa Cruz, CA). Signals were detected by using the ECL system (GE Healthcare, Buckinghamshire, U.K.). The integrated density (density in three different areas) of the bands was quantified by using NIH Image analysis software ver. 1.61.

Assessment of Apoptosis. Apoptotic cells were detected with TUNEL method by using an apoptosis detection kit (TaKaRa Bio, Shiga, Japan) as described in ref. 8. Semiquantitative analysis was performed by viewing random areas at a magnification of ×100 and scored for the number of apoptotic nuclei present in renal tissues. The mean number of positive-stained nuclei in at least 20 random fields was evaluated and expressed as the renal apoptotic score.

Determination of Superoxide Production in Renal Tissue. Superoxide production in renal tissue samples was detected by dihydroethidium conversion to ethidium, as described in ref. 32. Briefly, 4-μm-thick sections from each group were incubated in culture vessels containing endotoxin-free RPMI medium1640 culture with 2 μmol/l of dihydroethidium (Sigma–Aldrich) for 1 h at 37°C in the dark. After rinsing with PBS, the fluorescence at an excitation wavelength of 480 nm was detected with an emission wavelength of 610 nm by using confocal laser-scanning microscopy (TCS NT; Leica Microsystems, Tokyo, Japan).

Statistics. Values are given as mean $\pm$ SEM. All parameters were evaluated with the Mann–Whitney's U test or the Kruskal–Wallis test when multiple mean comparisons were made. Survival rate was measured by using the Kaplan–Meier method.

1. Kuro-o M, Matsumura Y, Aizawa H, Kawaguchi H, Suga T, Utsugi T, Ohyama Y, Kurabayashi M, Kaname T, Kume E, *et al.* (1997) *Nature* 390:45–51.
2. Kurosu H, Yamamoto M, Clark JD, Pastor JV, Nandi A, Gurnani P, McGuinness OP, Chikuda H, Yamaguchi M, Kawaguchi H, *et al.* (2005) *Science* 309:1829–1833.
3. Koh N, Fujimori T, Nishiguchi S, Tamori A, Shiomi S, Nakatani T, Sugimura K, Kishimoto T, Kinoshita S, Kuroki T, Nabeshima Y (2001) *Biochem Biophys Res Commun* 280:1015–1020.
4. Sugiura H, Yoshida T, Tsuchiya K, Mitobe M, Nishimura S, Shirota S, Akiba T, Nihei H (2005) *Nephrol Dial Transplant* 20:2636–2645.
5. Cho AR, Uchio-Yamada K, Torigai T, Miyamoto T, Miyoshi I, Matsuda J, Kurosawa T, Kon Y, Asano A, Sasaki N, Agui T (2006) *Mamm Genome* 17:407–416.
6. Ogura A, Asano T, Matsuda J, Takano K, Nakagawa M, Fukui M (1989) *Lab Anim* 23:169–174.
7. Takaki A, Jimi S, Segawa M, Iwasaki H (2004) *Ann N Y Acad Sci* 1011:332–338.
8. Satoh M, Kashihara N, Fujimoto S, Horike H, Tokura T, Namikoshi T, Sasaki T, Makino H (2003) *J Pharmacol Exp Ther* 305:1183–1190.
9. Mansouri A, Gaou I, De Kerguenec C, Amsellem S, Haouzi D, Berson A, Moreau A, Feldmann G, Letteron P, Pessayre D, Fromenty B (1999) *Gastroenterology* 117:181–190.
10. Satoh M, Fujimoto S, Haruna Y, Arakawa S, Horike H, Komai N, Sasaki T, Tsujioka K, Makino H, Kashihara N (2005) *Am J Physiol* 288:F1144–F1152.
11. Kanwar YS, Liu Z, Kumar A, Usman MI, Wada J, Wallner EI (1996) *J Clin Invest* 98:2478–2488.
12. Maser EJ (1995) in *Handbook of Physiology: Aging*, ed Masoro EJ (Oxford Univ Press, New York), Section 11:3–24.
13. Aizawa H, Saito Y, Nakamura T, Inoue M, Imanari T, Ohyama Y, Matsumura Y, Masuda H, Oba S, Mise N, *et al.* (1998) *Biochem Biophys Res Commun* 249:865–871.
14. Takeshita K, Fujimori T, Kurotaki Y, Honjo H, Tsujikawa H, Yasui K, Lee JK, Kamiya K, Kitaichi K, Yamamoto K, *et al.* (2004) *Circulation* 109:1776–1782.
15. Saito Y, Yamagishi T, Nakamura T, Ohyama Y, Aizawa H, Suga T, Matsumura Y, Masuda H, Kurabayashi M, Kuro-o M, Nabeshima Y, Nagai R (1998) *Biochem Biophys Res Commun* 248:324–329.
16. Fukino K, Suzuki T, Saito Y, Shindo T, Amaki T, Kurabayashi M, Nagai R (2002) *Biochem Biophys Res Commun* 293:332–337.
17. Nagai R, Saito Y, Ohyama Y, Aizawa H, Suga T, Nakamura T, Kurabayashi M, Kuro-o M (2000) *Cell Mol Life Sci* 57:738–746.
18. Saito Y, Nakamura T, Ohyama Y, Suzuki T, Iida A, Shiraki-Iida T, Kuro-o M, Nabeshima Y, Kurabayashi M, Nagai R (2000) *Biochem Biophys Res Commun* 276:767–772.
19. Baylis C (2006) *Nat Clin Pract Nephrol* 2:209–220.
20. Wang Y, Michikawa Y, Mallidis C, Bai Y, Woodhouse L, Yarasheski KE, Miller CA, Askanas V, Engel WK, Bhasin S, Attardi G (2001) *Proc Natl Acad Sci USA* 98:4022–4027.
21. Melov S, Hinerfeld D, Esposito L, Wallace DC (1997) *Nucleic Acids Res* 25:974–982.
22. Susztak K, Bottinger EP (2006) *J Am Soc Nephrol* 17:361–367.
23. Susztak K, Raff AC, Schiffer M, Bottinger EP (2006) *Diabetes* 55:225–233.
24. Gorin Y, Block K, Hernandez J, Bhandari B, Wagner B, Abboud HE (2005) *J Biol Chem* 280:39616–39626.
25. Haugen EN, Croatt AJ, Nath KA (2000) *Kidney Int* 58:144–152.
26. Yamamoto M, Clark JD, Pastor JV, Gurnani P, Nandi A, Kurosu H, Miyoshi M, Ogawa Y, Castrillon DH, Rosenblatt KP, Kuro-o M (2005) *J Biol Chem* 280:38029–38034.
27. Lebovitz RM, Zhang H, Vogel H, Cartwright J, Dionne L, Lu N, Huang S, Matzuk MM (1996) *Proc Natl Acad Sci USA* 93:9782–9787.
28. Blackwell KA, Sorenson JP, Richardson DM, Smith LA, Suda O, Nath KA, Katusic ZS (2004) *Am J Physiol* 287:H2448–H2453.
29. Kokoszka JE, Coskun P, Esposito LA, Wallace DC (2001) *Proc Natl Acad Sci USA* 98:2278–2283.
30. Kujoth GC, Hiona A, Pugh TD, Someya S, Panzer K, Wohlgemuth SE, Hofer T, Seo AY, Sullivan R, Jobling WA, *et al.* (2005) *Science* 309:481–484.
31. Nath KA (1992) *Am J Kidney Dis* 20:1–17.
32. Satoh M, Ogita H, Takeshita K, Mukai Y, Kwiatkowski DJ, Liao JK (2006) *Proc Natl Acad Sci USA* 103:7432–7437.